Clin Oral Invest (2012) 16:33–38
DOI 10.1007/s00784-010-0479-6

ORIGINAL ARTICLE

Counting touching cell nuclei using fast ellipse detection to assess in vitro cell characteristics: a feasibility study

Dan Dominik Brüllmann · Andreas Pabst · Karl M. Lehmann · Thomas Ziebart · Marc O. Klein · Bernd d'Hoedt

Received: 20 May 2010 / Accepted: 28 September 2010 / Published online: 15 October 2010
© Springer-Verlag 2010

Abstract In this article, we describe a new image analysis software that allows rapid segmentation and separation of fluorescently stained cell nuclei using a fast ellipse detection algorithm. Detection time ranged between 1.84 and 3.14 s. Segmentation results were compared with manual evaluation. The achieved over-segmentation rate was 0.11 (0.1 double counts and 0.01 false positive detections), and the under-segmentation rate was of 0.03 over all images. We demonstrate the applicability of the proposed algorithm to automated counting of fluorescent-labeled cell nuclei and to tissue characterization. Moreover, the performance of the proposed algorithm is compared with preexisting automated image analysis techniques described by others.

Keywords Image analysis · Computer-assisted · Cell number · Cell density · Fibroblasts

D. D. Brüllmann (✉) · B. d'Hoedt
Department of Oral Surgery, University Medical Center of the Johannes Gutenberg University Mainz,
Augustusplatz 2,
55131 Mainz, Germany
e-mail: bruellmd@mail.uni-mainz.de

A. Pabst · T. Ziebart · M. O. Klein
Department of Oral and Maxillofacial Surgery, University Medical Center of the Johannes Gutenberg University Mainz,
Augustusplatz 2,
55131 Mainz, Germany

A. Pabst
e-mail: andreas.pabst@web.de

T. Ziebart
e-mail: ziebart@mkg.klinik.uni-mainz.de

M. O. Klein
e-mail: klein@mkg.klinik.uni-mainz.de

K. M. Lehmann
Department of Prosthodontics, University Medical Center of the Johannes Gutenberg University Mainz,
Augustusplatz 2,
55131 Mainz, Germany
e-mail: lehmann@prothetik.klinik.uni-mainz.de

Introduction

High-throughput microscopic imaging technology provides enormous amounts of digital image data, involving potentially thousands of images to be analyzed for each assay. Thus, manual evaluation can be time consuming. The main advantage of computer-based image analysis is that a large amount of visual data may be processed in a short period of time [1–5]. However, it is essential that the analyzed images are well standardized to obtain reliable results. This concerns imaging parameters, such as contrast and magnification during the acquisition process, as well as standard preparation of cell assays. Simple imaging techniques, such as thresholding and simple edge detection, are inadequate if cells overlap. Thus, the user must ensure that cells do not overlap in cultures, or algorithms for the separation of touching cells in images must be used [6, 7].

In this report, we describe a simple method for separating touching cell nuclei using a fast ellipse detection method, adapted from a Hough transform. The proposed method uses fluorescence imaging in which cell nuclei are visualized by a special fluorescent stain to visualize cell nuclei (human fibroblasts were used). Touching cell nuclei are separated by an adapted ellipse detection algorithm. The results obtained can either be used for cell counting appliances or characterization of tissue, using Voronoi diagrams or Delaunay triangulation.

Methods

Surface samples

One type of biocompatibility measurement was performed on feldspathic ceramic VM13 (VITA Zahnfabrik, H. Rauter GmbH & Co. KG, Bad Säckingen, Germany). The samples were disk-shaped (diameter, 12±0.5 mm; thickness, 2±0.5 mm). Other biocompatibility growth tests were performed on sand-blasted and autoclaved titanium plates, supplied by the Institut Straumann (Basel, Switzerland). Sheets of grade 2 unalloyed Ti (ASTM F67 "unalloyed Ti for surgical implant applications," 1 mm in thickness) were punched to a diameter of 15 mm. Disks were degreased by washing in acetone and processing through a 2% ammonium fluoride/2% hydrofluoric acid/10% nitric acid solution at 55°C for 30 s. Before use, the disks were washed, sonicated, and sterilized in an oxygen plasma cleaner (PDC-32 G, Harrick Plasma, Ithaca, NY).

Cell cultures

Fibroblast culture assay

Human gingival fibroblasts (Lonza, Basel, Switzerland; no. CC-7049) were cultured in an incubator with 5% CO_2 and 95% air at 37°C. Cells were passaged at regular intervals, depending on their growth characteristics, using 0.25% trypsin (Seromed Biochrom, Berlin, Germany). Fibroblasts were grown in stromal cell growth medium (Lonza, Basel, Switzerland) with a 1% penicillin–streptomycin–neomycin antibiotic mixture, 10% fetal calf serum (FCS), and 500 ng basic fibroblast growth factor per 500 mL medium. The cells were transferred to the ceramic and titanium samples and incubated for 24 h. Vital staining of the cells was performed with a green cell tracker (Molecular Probes, Invitrogen, Karlsruhe, Germany), according to the manufacturer's staining protocol. Stock solution (15 μL) was added to 100,000 cells suspended in 5 mL basal medium. After 30 min of incubation at room temperature, cells were centrifuged and further processed. Preliminary studies revealed stable fluorescence activity over at least 72 h. Cell nuclei were then stained using 4′,6-diamidin-2′-phenlindoldihydrochloride (Roche Diagnostics GmbH, Mannheim, Germany).

EPC culture assay

Mononuclear endothelial progenitor cells (EPCs) were isolated by density gradient centrifugation with Biocoll (Biochrom KG, Berlin, Germany) from peripheral blood of healthy human volunteers as previously described [8]. Immediately following isolation, total MNCs (8×106 cells per milliliter of medium) were plated on 6-well plates with human fibronectin (Sigma, Steinheim, Germany) and maintained in EBM supplemented with EGM SingleQuots, VEGF (100 ng/mL), and 20% FCS. Different bisphosphonates (clodronate, pamidronate, and ibandronate) were added in a concentration of 50 μmol. No bisphosphonates were added to the control group. After 72 h, EPC were stained. Vital staining of the osteogenic cells was performed with green cell tracker (Molecular Probes, Invitrogen, Karlsruhe, Germany) according to the manufacturer's staining protocol. Fifteen microliters of the stock solution was added to 5 ml basal medium. After 30 min of incubation at room temperature, cells were washed with basal medium and microscopic evaluation proceeded.

Image acquisition

To assess counting accuracy, cell cultures were photographed under a light microscope at 20× magnification using a Zeiss AcioCam MRC camera (Zeiss MicroImaging GmbH, Göttingen, Germany) with 4.45-μm physical pixels at 2×2 binning mode. Three cultures were cultivated: one for counting tests on standard culture dishes and two for assessment of growth characteristics by means of increasing cell numbers and total covered areas after 72, 84, and 96 h.

Image segmentation

Because the two different staining methods used here produced fluorescent images at different wavelengths, cell soma were gathered in the green channel of the RGB images, while cell nuclei were visible in the blue channel. Thus, cell nuclei images were gathered by copies of the blue channel of acquired images to 8-bit gray-level images. Centroids of the cells' nuclei were then detected by calculating the derivatives of the image g in the x- and y-directions (g_x and g_y) using sobel masks:

$$g_x = g \times \begin{pmatrix} 1 & 0 & -1 \\ 2 & 0 & -2 \\ 1 & 0 & -1 \end{pmatrix} \qquad g_y = g \times \begin{pmatrix} 1 & 2 & 1 \\ 0 & 0 & 0 \\ -1 & -2 & -1 \end{pmatrix} \tag{1}$$

A gradient image d was calculated of these derivatives:

$$d = \sqrt{g_x^2 + g_y^2} \tag{2}$$

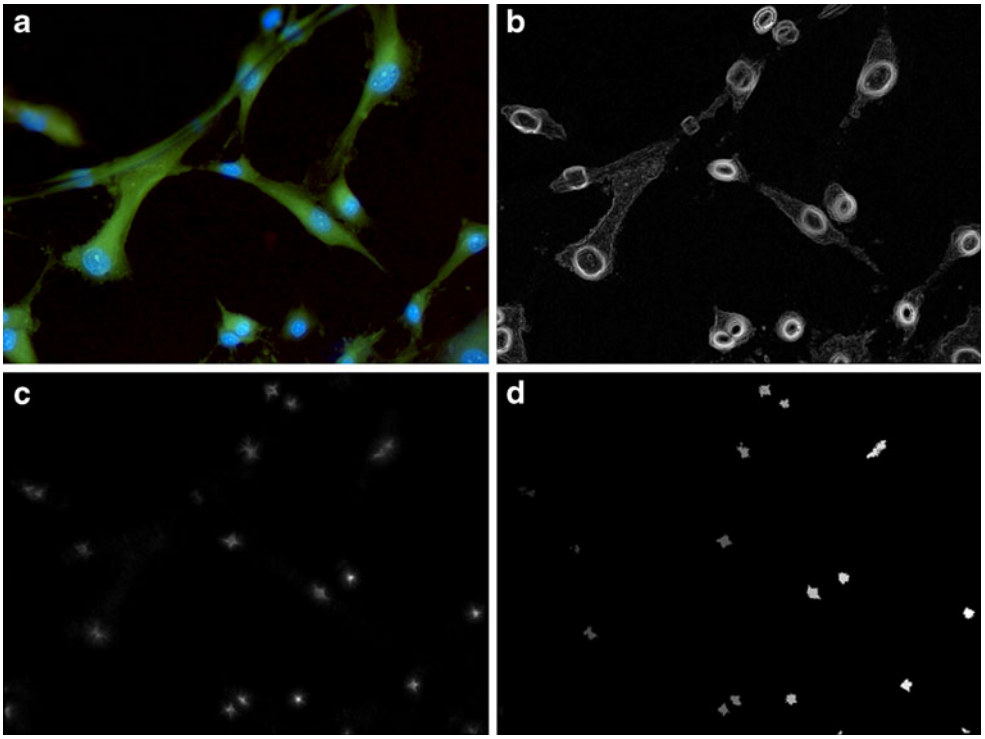

Fig. 1 Original image (**a**) and the derived edge magnitude (**b**). The nucleus centers are accumulated in parameter space (**c**) for labeling (**d**)

Then, a binary image of g was calculated using a simple threshold t_1 to obtain the edge pixel candidates E_h (x, y) of the cells and nuclei.

$$d(x,y) \rightarrow E_h(x,y)\begin{cases} 1 & if \quad d > t_1 \\ 0 & else \end{cases} \tag{3}$$

Then, the nuclei's centroids c_i (x_c, y_c) were detected by accumulating them in a two-dimensional parameter space using the following equation [9, 10]:

$$\begin{aligned} x_c &= x_e - R(g_x/g) \\ y_c &= y_e - R(g_y/g) \end{aligned} \tag{4}$$

The parameter space P (x_{ci}, y_{ci}) was scanned for maxima above the scan threshold t_2. If one of these was reached, the corresponding area was labeled by a seed fill procedure, and the segmented region's centroid was saved as location of a cell nucleus (Fig. 1d). For quantification of cell growth characteristics, cell size was measured in the green channel of RGB images using a threshold method described by Zinnreich et al. to count the size of area covered by the cells visible in the image [11].

Results

In total, 40 images were evaluated using the software. The image size was 1388 × 1040 pixels (Fig. 2a and b). Detection time ranged from 1.84 to 3.14 s (median, 2.07 s; standard deviation, 0.17) and correlated with the number of cells in the image (Fig. 3). Software results were printed and evaluated visually by performing manual counts. The proposed method also separated touching nuclei of circular, elliptical, and ovoid shapes. Over all images, the software

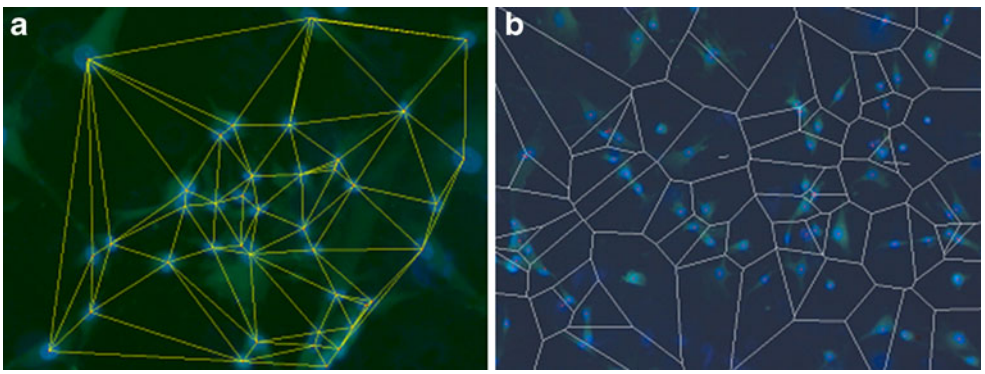

Fig. 2 Derived Delaunay triangulation and Voronoi diagram using the calculated centroids as seen on the fibroblast culture assay

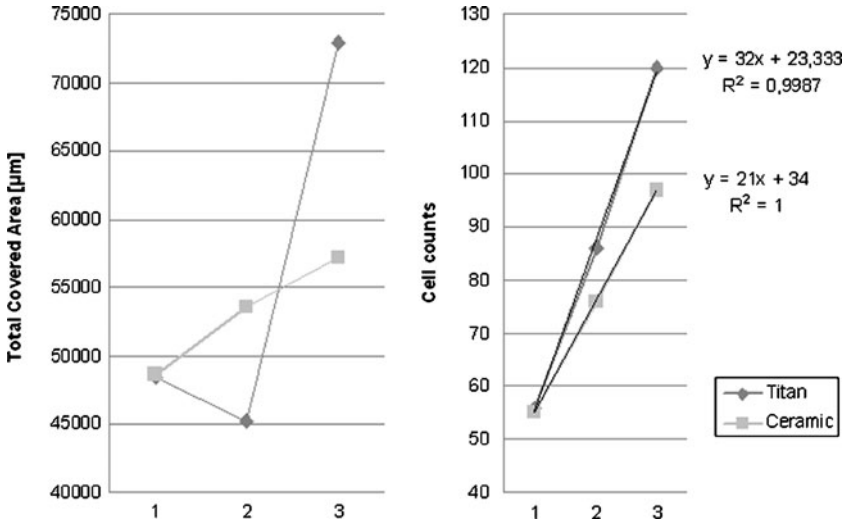

Fig. 3 Change of cell size (Total Covered Area) as seen in the Fibroblast culture assay and cell counts over three time periods after 72 h (*1*), 84 h (*2*), and 96 h (*3*)

achieved an over-segmentation rate of 0.11 (0.1 double counts and 0.01 false positive detections) and an under-segmentation rate of 0.03 (Table 1).

The software performed an average of 3.95 double counts per image (median, 3; standard deviation, 3.89; minimum, 0; maximum, 18). An average of 0.39 false positive detections were performed per image (median, 0; standard deviation, 1.14; maximum, 6). False negative detections occurred at an average of 1.29 counts per image (median, 1; standard deviation, 1.05; maximum, 5).

Growth tests revealed different growth characteristics of cells on titanium vs. ceramic plates. Cell counts on ceramic plates increased more slowly than on titanium plates, from 55 to 76 after 72 h and 97 after 84 h. The total covered area increased from 48,659.9 to 53,619.8 μm^2 and to 57,172.5 μm^2. As expected, the average cell size decreased, from 1,787.3 to 1,425.3 μm^2 and to 1,190.72 μm^2 after 24 h. Cell size and numbers growing on titanium plates showed a different behavior: cell counts increased, from 56 to 86 after 84 h and to 120 after 96 h. The total covered area increased, from 48,408.5 to 45,282.1 μm^2 after 84 h and to 72,990.7 μm^2 after 84 h on titanium plates. The average cell sizes decreased from 1,746.3 to 1,063.70 μm^2 after 84 h and to 1,228.8 μm^2 after 96 h (see Fig. 3).

Inhibition tests with EPC showed 145 cell counts performed by the software vs. 150 cells counted by the observer for cells cultivated in the raw culture media. For culture media incubated with ibandronate, the software found 149 cell counts; the same value was counted by the observer. In the culture well incubated with pamidronate, the software counted 78 cells after 72 h vs. 80 cells counted by the observer and indicated a significant cleavage inhibition for pamidronate (see Fig. 4). Analysis of the area in the images totally covered by the cells revealed difference of the total covered area of initially 73,794 pixels for the raw culture and 81,602 pixels for the cells cultured in ibandronate containing media and 30,989 for pamidronate, respectively (see Fig. 4).

Discussion

Different algorithms for separation of touching cells or cell nuclei have been described [12–14]. The achieved over-segmentation rate of 0.11 (0.1 double counts and 0.01 false positive detections) and under-segmentation rates of 0.03 over all images correspond to the rates achieved by Li et al. [12] for under-segmentation. Bernard et al. correctly identified mammalian fibroblasts 91% of

Table 1 Statistical evaluation of the software's counting performance

	Hand count	Double counts	False positive	False negative
Mean		3.95	1.05	1.29
Median		3	0	1
Standard deviation		3.89	1.137	1.05
Minimum		0	0	0
Maximum		18	6	5
Sum	1,615	162	16	53
Percent	100	0.10	0.01	0.03

Manual counts were used as gold standard

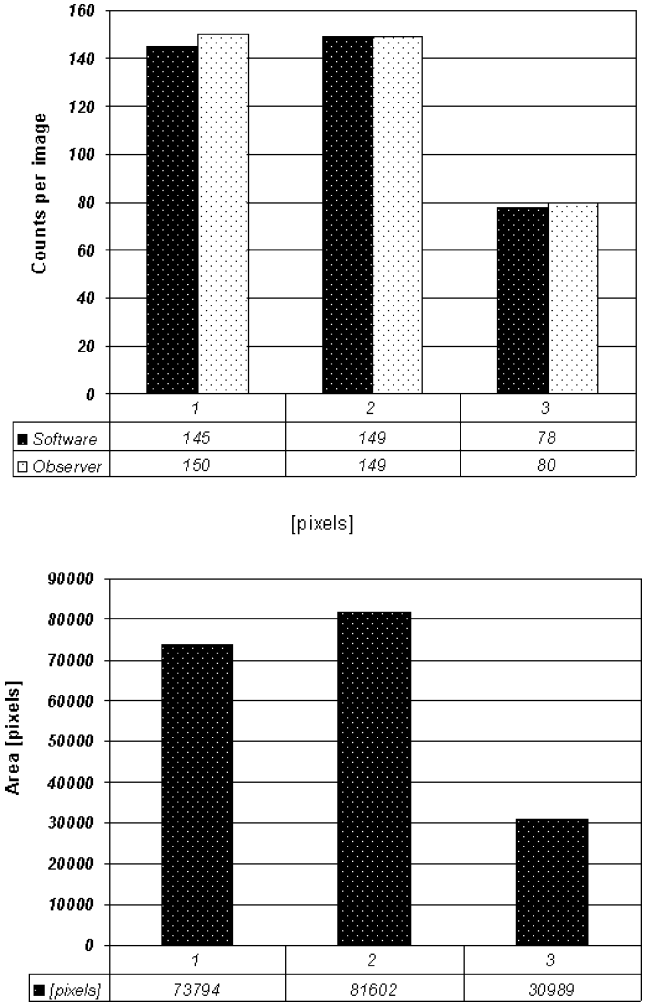

Fig. 4 Change of cell size and cell counts during inhibition test with EPCs as seen after a time period of 72 h. Only slight differences were seen between the raw culture media (*1*) and the one containing ibandronate (*2*). The result indicated a significant cleavage inhibition for pamidronate as seen by the significant lower number of cells counted in the image (*3*)

the time in a model-based automated detection algorithm [14, 15]. Pal et al. accurately identified cells 82% of the time when comparing their algorithm using dominant contour feature points with manual evaluation [7]. A major problem in our proposed method is double segmentation. However, we think that double counts could be lowered by smoothing the parameter space prior to maxima detection or by implementing distance constraints. However, the algorithm proposed here proved its ability to detect blue cell nuclei (as shown in the fibroblast culture) as well as green round cell soma in the inhibition tests with the EPC assay. In both assays, the predicted effect was evidently shown: the growth test showed an increase in cell number and covered area, whereas inhibition test with pamidronate showed a decrease in cell number and size of the covered area (Fig. 4).

The proposed segmentation algorithm for cell nuclei or round cells can be used for the assessment of tissue characteristics during growth or pathological classification. Centroids of cell nuclei can be used for the quantification of tissue characteristics, based on distribution of cell nuclei using Delaunay triangulation or cell separation using watershed [6] transformation or Voronoi diagrams. As an example, we used the algorithm described by Bourke [16] for a fast calculation of Delaunay triangulation. In a set $V = \{v_1, \ldots, v_N\}$ of points, any edge spanned by v_h, v_i, and v_j is a Delaunay edge if and only if there exists a point x such that the circle centered at x and passing through v_h, v_i, and v_j does not contain in its interior any other point v [17]. Based on the acquired Delaunay graph, descriptive measures that characterize tissue or cell cultures can be calculated [18]. Theoretical frameworks defining generalized finite Voronoi neighborhoods are proposed to serve as heterogeneous generators of the resulting model tissue, and simulations of the position of cell centers showed the feasibility of Voronoi methods generating realistic cell shapes [19]. However, if cell separation using approximated graphs derived from Delaunay triangulation and Voronoi diagrams are inspected visually (Fig. 4a, b), it seems that Voronoi diagrams are not always exact for cell separation in growing tissues. Correlation between diagrams and cell borders may be more exact in areas where cells are in close contact and at short distances from each other. Thus, separation of touching cells might only be valid for densely packed cells (Fig. 5).

As a summary, the developed software allows fast and uncomplicated quantification of initial cell number and average size. Thus, it can serve as a reliable tool for biocompatibility screening of surface modifications. We think that the segmentation of cell nuclei can be easily adapted for the counting of touching cells of circular, elliptical, and ovoid shapes.

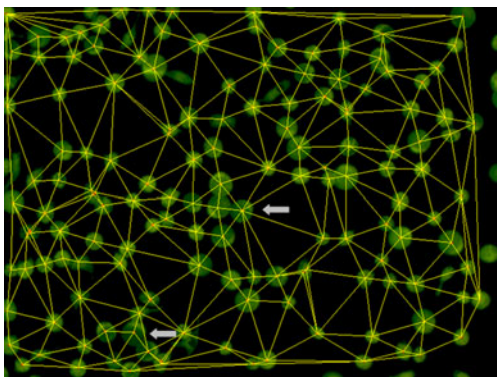

Fig. 5 Derived Delaunay triangulation using the calculated centroids as seen on the EPC culture assay. Even for structure with other color, the software is able to separate the touching round structures (see *arrows*)

Acknowledgements All authors disclose any actual or potential conflict of interest including any financial, personal, or other relationships with other people or organizations within that could inappropriately influence this work.

References

1. Brüllmann DD, Klein MO et al (2009) Implementation of new software for fast screening of cell compatibility on surface modifications using low-contrast time-lapsed microscopy. Clin Oral Investig. doi:10.1007/s00784-009-0339-4
2. Debeir O, Camby I, Kiss R, Van Ham P, Decaestecker C (2004) A model-based approach for automated in vitro cell tracking and chemotaxis analyses. Cytometry 60:29–40
3. Ersoy I, Palaniappan K (2008) Multi-feature contour evolution for automatic live cell segmentation in time lapse imagery. Conf Proc IEEE Eng Med Biol Soc 1:371–374
4. Fenistein D, Lenseigne B, Christophe T, Brodin P, Genovesio A (2008) A fast, fully automated cell segmentation algorithm for high-throughput and high-content screening. Cytometry 73:958–964
5. Sacan A, Ferhatosmanoglu H, Coskun H (2008) Cell track: an open-source software for cell tracking and motility analysis. Bioinformatics 24:1647–1649
6. Mao KZ, Zhao P, Tan PH (2006) Supervised learning-based cell image segmentation for p53 immunohistochemistry. IEEE Trans Biomed Eng 53:1153–1163
7. Pal U, Rodenacker K, Chaudhuri BB (1998) Automatic cell segmentation in cyto- and histometry using dominant contour feature points. Anal Cell Pathol 17:243–250
8. Ziebart T, Yoon CH, Trepels T et al (2008) Sustained persistence of transplanted proangiogenic cells contributes to neovascularization and cardiac function after ischemia. Circ Res 103:1327–1334
9. Brüllmann D, Mennickheim J, d'Hoedt B (2009) Fast algorithm for detection of reference spheres in digital panoramic radiography. Comput Biol Med 39:615–619
10. Davies E (2005) Machine vision: theory, algorithms, practicalities. Elsevier, Amsterdam
11. Zack GW, Rogers WE, Latt SA (1977) Automatic measurement of sister chromatid exchange frequency. J Histochem Cytochem 25:741–753
12. Li G et al (2008) Segmentation of touching cell nuclei using gradient flow tracking. J Microsc 231:47–58
13. Ranefal P et al (1997) A new method for segmentation of colour images applied to immunohistochemically stained cell nuclei. Anal Cell Pathol 15:145–156
14. Selinummi J et al (2009) Bright field microscopy as an alternative to whole cell fluorescence in automated analysis of macrophage images. PLoS ONE 4:e7497
15. Bernard R, Kanduser M, Pernus F (2001) Model-based automated detection of mammalian cell colonies. Phys Med Biol 46:3061–3072
16. Bourke P (1989) Efficient triangulation algorithm suitable for terrain modelling. Pan Pacific Computer Conference, Beijing
17. Lee D, Schachter J (1980) Two algorithms for constructing a Delaunay triangulation. Int J Comput Inf Sci 9:219–242
18. Sudbo J, Marcelpoil R, Reith A (2000) New algorithms based on the Voronoi diagram applied in a pilot study on normal mucosa and carcinomas. Anal Cell Pathol 21:71–86
19. Bock M et al (2010) Generalized Voronoi tessellation as a model of two-dimensional cell tissue dynamics. B Math Biol 72:1696–1731

Copyright of Clinical Oral Investigations is the property of Springer Science & Business Media B.V. and its content may not be copied or emailed to multiple sites or posted to a listserv without the copyright holder's express written permission. However, users may print, download, or email articles for individual use.